Backscatter Modulation Design for Symbiotic Radio Networks

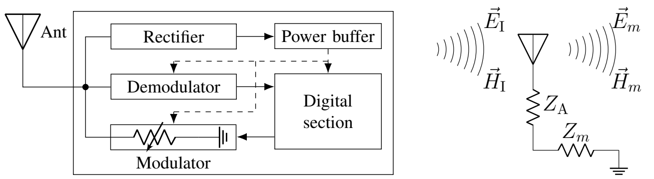

(a) Block diagram of a passive tag (b) Backscatter modualtion

Fig. 1. For a passive tag, the rectifier and demodulator rely on the incident electromagnetic wave for energy harvesting and source decoding, while the load-switcher adjusts the reradiated signal for backscatter modulation.

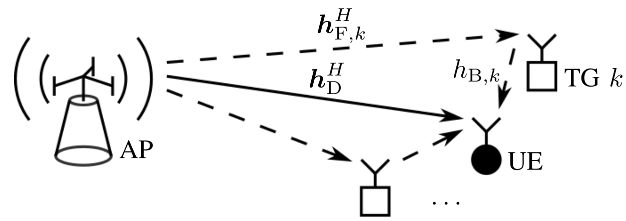

Fig. 2. A single-user multi-tag symbiotic radio system.

I. Backscatter Model

A. Backscatter Principles

A bistatic backscatter system consists of an excitation source, multiple (semi-)passive tags, and a backscatter reader. When illuminated, the tags simultaneously harvest energy, backscatter message, and demodulate the source signal if necessary. Fig. 1(a) shows a typical passive with a scattering antenna, an energy harvester, an integrated receiver[1], a load-switching modulator, and on-chip components (e.g., micro-controller, memory, and sensors). A portion of the impinging signal is absorbed by the tag while the remaining is backscattered to the space. According to Green's decomposition [2], the backscattered signal can be decomposed into the *structural mode* component and the *antenna mode* component. The former is fixed and depends on the antenna geometry and material properties[2], while the latter is adjustable and depends on the mismatch of the antenna and load impedance. Fig. 1(b) illustrates a simplified circuit and backscatter model at tag state m. The corresponding reflection coefficient is defined as[3]

$$\Gamma_m = \frac{Z_m - Z_{\mathrm{A}}^*}{Z_m + Z_{\mathrm{A}}}, \tag{1}$$

where Z_m is the load impedance at state m and Z_{A} is the antenna input impedance.

B. Backscatter Modulation

Backscatter modulation is achieved by switching the tag load impedance between different states. For an M-ary Quadrature Amplitude Modulation (QAM) at state $m \in \mathcal{M} \triangleq \{1, \ldots, M\}$, the reflection coefficient Γ_m maps to the signal constellation point $\bar{c}_m$ as [5]

$$\Gamma_m = \alpha \frac{\bar{c}_m}{\max_{m'} |\bar{c}_{m'}|}, \tag{2}$$

where $\alpha \in [0, 1]$ is the reflection efficiency at a given direction. For simplicity, we consider an M-ary Phase Shift Keying (PSK) with constellation set $\mathcal{C} \triangleq \{\bar{c}_1, \ldots, \bar{c}_M\}$, where the m-th constellation point is

$$\bar{c}_m = \exp\left(j \frac{2\pi m}{M}\right). \tag{3}$$

Remark 1. *For passive tags, the reflection efficiency α controls the tradeoff between the harvestable power and backscatter strength: $\alpha = 0$ corresponds to maximum power transfer to the tag, while $\alpha = 1$ with M-PSK corresponds to ideal Intelligent Reflecting Surface (IRS) with M discrete states.*

II. Backscatter Detection and Achievable Rates

A. System Model

As shown in Fig. 2, we propose a single-user (UE) multi-tag (TG) symbiotic radio network where the Radio Frequency (RF) signal generated by the Q-antenna Access Point (AP) is shared by two coexisting systems. In the primary downlink system, the AP transmits information to the single-antenna user. In the secondary backscatter system, the AP acts as the carrier emitter, the K nearby single-antenna tags modulate their information over the reradiated RF signals, and the user serves as the multi-tag backscatter reader. Denote the AP-UE direct channel as $\boldsymbol{h}_{\mathrm{D}}^H \in \mathbb{C}^{1\times Q}$, the AP-TG $k \in \mathcal{K} \triangleq \{1, \ldots, K\}$ forward channel as $\boldsymbol{h}_{\mathrm{F},k}^H \in \mathbb{C}^{1\times Q}$, the TG k-UE backward channel as $h_{\mathrm{B},k}$, and the cascaded forward-backward channel of tag k as $\boldsymbol{h}_{\mathrm{C},k}^H \triangleq h_{\mathrm{B},k} \boldsymbol{h}_{\mathrm{F},k}^H \in \mathbb{C}^{1\times Q}$. For simplicity, we consider a quasi-static block fading model where the channel coefficients remain constant within each coherence interval and vary independently over different coherence intervals, and assume the coherence interval T is much longer than the backscatter symbol period T_c and primary symbol period T_s. We also assume the direct channel and all cascaded channels can be successfully estimated

[1]For example, [1] prototyped a compact-size pulse position demodulator based on an envelope detector, which brings great potential to coordination, synchronization, and reflection pattern control.

[2]The structural mode component can be regarded as part of the environment multipath and modeled by channel estimation [3].

[3]We assume the linear backscatter model where the reflection coefficient is irrelevant to the incident electromagnetic field at the tag [4].

and fed back to the AP.[4] Since the tags need to physically switch the loads for backscatter modulation, they communicate at a much longer symbol period (and lower rates) than the primary system. As such, we assume the transitions of all tags are perfectly synchronized, and the backscatter symbol period satisfies $T_c = NT_s$ where $N \gg 1$ is a positive integer.

Without loss of generality, we focus on the transmissions and detections during one particular backscatter symbol period. To provide a preliminary insight, we assume the primary symbol $s[n]$ at block $n \in \mathcal{N} \triangleq \{1, \ldots, N\}$ is in standard Circularly Symmetric Complex Gaussian (CSCG) distribution, and the backscatter symbol c_k of tag k employs M-PSK modulation by (3), i.e., $c_k \in \mathcal{C}$, $\forall k \in \mathcal{K}$. Thus, the signal received by the user at block n can be expressed as[5]

$$y[n] = \left(\boldsymbol{h}_{\mathrm{D}}^H + \sum_{k \in \mathcal{K}} \sqrt{\alpha_k} \boldsymbol{h}_{\mathrm{C},k}^H c_k \right) \boldsymbol{w} s[n] + w[n], \qquad (4)$$

where $\boldsymbol{w} \in \mathbb{C}^{Q \times 1}$ is the active precoder satisfying $\|\boldsymbol{w}\|^2 \leq P$, P is the average transmit power constraint at the AP, and $w[n] \sim \mathcal{CN}(0, \sigma_w^2)$ is the equivalent Additive White Gaussian Noise (AWGN) at block n. Besides, we collect the backscatter symbols of K tags into $c_{\mathcal{K}} \triangleq \{c_k : k \in \mathcal{K}\}$, stack the received signal over N blocks as $\boldsymbol{y} \triangleq [y[1], \ldots, y[N]]^T \in \mathbb{C}^{N \times 1}$, and define the equivalent channel for primary transmission as

$$\boldsymbol{h}_{\mathrm{E}}^H(c_{\mathcal{K}}) \triangleq \boldsymbol{h}_{\mathrm{D}}^H + \sum_{k \in \mathcal{K}} \sqrt{\alpha_k} \boldsymbol{h}_{\mathrm{C},k}^H c_k. \qquad (5)$$

Remark 2. *The proposed symbiotic radio system includes a multiplicative Multiple Access Channel (MAC) where the AP and the tags simultaneously transmit to the user. It inspired [TODO] to perform Successive Interference Cancellation (SIC) that first non-coherently detects the primary message under backscatter uncertainty, then cancels its contribution and decodes the tag messages. This scheme requires non-coherent coding at the AP and K re-encoding, precoding, and subtraction operations at the user. However, different from the conventional MAC with Superposition Coding (SC), the symbiotic radio system involves Multiplication Coding (MC) that combines the primary and secondary messages by multiplication. Hence, novel multi-stream detection techniques should be tailored to symbiotic radio systems to accommodate the massive connectivity of tags and the multiplicative combination of links.*

B. Backscatter Detection

To reveal the impact of backscatter modulation on the primary transmission and avoid the exponential complexity of joint detection, we extend the non-coherent Ambient Backscatter Communications (AmBC) detection [11] to the multi-tag case, and propose a low-complexity energy detection to decode the backscatter symbols under primary source uncertainty. It requires no dedicated receivers or non-coherent codes at the AP, and can be readily implemented over legacy downlink systems.

Remark 3. *One key property of symbiotic radio is the primary message propagates to the user from a known channel and multiple multiplicative channels with uncertainty introduced by backscatter modulation. As such, each reflection coefficient simultaneously encodes the tag message and influences the equivalent channel of the primary link. If the backscatter symbols can be successfully decoded first, they can be modeled within the equivalent channel* (5) *as in channel training, instead of being removed by SIC.*

To explicitly specify the instances of the backscatter symbols, we define the modulation index set as $m_{\mathcal{K}} \triangleq \{m_k \in \mathcal{M} : k \in \mathcal{K}\}$ and label the corresponding tag input combination as $\bar{c}_{m_{\mathcal{K}}} \triangleq \{\bar{c}_{m_k} \in \mathcal{C} : m_k \in \mathcal{M}, k \in \mathcal{K}\}$. Since any $\bar{c}_{m_{\mathcal{K}}}$ remains constant per N primary symbols, the received signal at block n is only subject to the variation of the primary source $s[n]$ and AWGN $w[n]$, and thus follows CSCG distribution $y_{m_{\mathcal{K}}}[n] \sim \mathcal{CN}\left(0, \sigma_{m_{\mathcal{K}}}^2\right)$, where the variance

$$\sigma_{m_{\mathcal{K}}}^2 = \Bigg| \underbrace{\left(\boldsymbol{h}_{\mathrm{D}}^H + \sum_{k \in \mathcal{K}} \sqrt{\alpha_k} \boldsymbol{h}_{\mathrm{C},k}^H \bar{c}_{m_k} \right)}_{\boldsymbol{h}_{\mathrm{E}}^H(\bar{c}_{m_{\mathcal{K}}})} \boldsymbol{w} \Bigg|^2 + \sigma_w^2, \qquad (6)$$

denotes the expectation of the received power per primary block under tag modulation index set $m_{\mathcal{K}}$. For the ease of exposition, we denote the hypothesis that the tag input combination at state $i \in \mathcal{I} \triangleq \{1, \ldots, M^K\}$ as $\mathcal{H}_i$, sort $\{\sigma_{m_{\mathcal{K}}}^2\}$ in ascending order by a one-to-one mapping $m_{\mathcal{K}} \mapsto i$,[6] define the received signal energy over N primary blocks as $z \triangleq \|\boldsymbol{y}\|^2$, and let $f(z \mid \mathcal{H}_i)$ be the conditional probability density function of receiving z under hypothesis $\mathcal{H}_i$. Correspondingly, z is the sum of N i.i.d. exponential variables each with mean σ_i^2, and the conditional probability density function follows Erlang distribution with shape N and scale σ_i^2 as[7]

$$f(z \mid \mathcal{H}_i) = \frac{z^{N-1} e^{-z/\sigma_i^2}}{\sigma_i^{2N} (N-1)!}. \qquad (7)$$

Remark 4. *The backscatter links essentially form a discrete-input continuous-output memoryless channel. To further reduce decoding complexity, we apply hard-decision detection and construct a Discrete Memoryless Thresholding Channel (DMTC), whose capacity is a function of both input distribution and decision thresholds [12].*

To maximize the mutual information for a general non-binary-input continuous-output channel, not only the decision region design remains an open problem, but also the optimal number of decision thresholds is still unknown. The reason is that the optimal decision region $\mathcal{R}_j$ of hypothesis $\mathcal{H}_j$ may be non-convex (i.e., consist of more than one disjoint partitions). The authors of [13] showed that any optimal quantizer with

[4]Due to the lack of RF chains at the passive tag, accurate and efficient Channel State Information (CSI) acquisition at the AP can be challenging. One possible approach is that the AP sends pre-defined pilots, the tags respond in well-designed manners, and the user performs least-square estimation with feedbacks [6]–[8].

[5]We omit the signal reflected by two or more times [9] and assume the time difference of arrival from different paths are negligible [10].

[6]When more than one modulation index sets yield the same energy level, the mapping is not unique and the detection fails to separate them. This blind spot issue can be potentially mitigated by multi-antenna techniques and is beyond the scope of this paper.

[7]In some papers, it may also be referred to as Gamma distribution.

arbitrary cost function must separate the backward channel (i.e., posterior distribution) into convex decision regions, and provided an upper bound on the number of thresholds.

Theorem 1. *If any L-input ($L \in \mathbb{Z}_{++}$) continuous-output channel follows Erlang distribution* (7)*, then the optimal number of thresholds is $L+1$ and the capacity-achieving decision region j has convex structure $\mathcal{R}_j^\star = [t_{j-1}^\star, t_j^\star)$.*

Proof. For any finite number of thresholds $S \in \mathbb{Z}_{++}$, let $\boldsymbol{t} \triangleq [t_0, \ldots, t_S]^T \in \mathbb{R}_+^{S \times 1}$ be the thresholding vector where $t_{s-1} < t_s$, $\forall s \in \mathcal{S} \triangleq \{1, \ldots, S\}$.[8] Denote the decision partition s as $R_s \triangleq [t_{s-1}, t_s)$. Without loss of generality, we assume $\mathcal{R}_j = \bigcup_{s \equiv j \pmod L} R_s$.[9] The thresholding design problem can be expressed as

$$\max_{\boldsymbol{t}} \quad I_{\mathrm{B}}(c_{\mathcal{K}}; z) \tag{8a}$$

$$\text{s.t.} \quad t_{s-1} < t_s, \quad \forall s \in \mathcal{S}. \tag{8b}$$

Problem (8) is intricate due to the strict inequality constraint (8b). Following [14], we first relax it to the convex counterpart, then discard the solutions that violate the original constraints. The Lagrangian function for the relaxed problem is

$$L(\boldsymbol{t}, \boldsymbol{\mu}) = -I_{\mathrm{B}}(c_{\mathcal{K}}; z) + \sum_{s \in \mathcal{S}} \mu_s (t_{s-1} - t_s), \tag{9}$$

where μ_s is the Lagrange multiplier associated with the non-strict version of (8b) and $\boldsymbol{\mu} \triangleq [\mu_1, \ldots, \mu_S]^T \in \mathbb{R}^{S \times 1}$. The corresponding Karush–Kuhn–Tucker (KKT) conditions on the optimal primal and dual solutions are, $\forall s \in \mathcal{S}$,

$$-\nabla_{t_s^\star} I_{\mathrm{B}}^\star(c_{\mathcal{K}}; z) + \mu_{s-1}^\star - \mu_s^\star = 0, \tag{10a}$$

$$\mu_s^\star \geq 0, \tag{10b}$$

$$\mu_s^\star (t_{s-1}^\star - t_s^\star) = 0. \tag{10c}$$

For DMTC based on energy detection (7), it is trivial to conclude $t_0^\star = 0$ and $t_S^\star = \infty$. Besides, since $t_{s-1} < t_s$ by definition, (10b) and (10c) imply $\mu_s^\star = 0$, $\forall s \in \mathcal{S}$. As such, $\forall s' \in \mathcal{S} \setminus \{S\}$, (10) reduces to

$$\nabla_{t_{s'}^\star} I_{\mathrm{B}}^\star(c_{\mathcal{K}}; z) = 0, \tag{11}$$

which can be explicitly written as

$$\sum_l P(x_l) \log \frac{P(z_j)}{P(z_{j+1})} \frac{P(z_{j+1} \mid x_l)}{P(z_j \mid x_l)} f(h_s \mid x_l) = 0, \tag{12}$$

where $j \equiv s \pmod L$. We notice that for a given j, $a_l \triangleq P(x_l) \log \frac{P(z_j)}{P(z_{j+1})} \frac{P(z_{j+1}|x_l)}{P(z_j|x_l)}$ is a constant for all $s \equiv j \pmod L$. Plugging (7) into (12), we have

$$\sum_l a_l e^{-h_s/\sigma_l^2} = 0, \tag{13}$$

which by Rolle's theorem has at most $L-1$ distinct real roots if $\sigma_i^2 \neq \sigma_j^2$, $i, j \in \mathcal{L}$. □

Once the decision region is determined, the discrete memoryless MAC can be recast as an equivalent point-to-point Discrete Memoryless Channel (DMC) from tag input combination alphabet $\mathcal{I}$ to output energy level alphabet $\mathcal{I}$. The the probability of receiving energy level j under tag input combination i is[10]

$$P(\bar{z}_j \mid \bar{c}_i) = P(z \in \mathcal{R}_j \mid \mathcal{H}_i) = \int_{\mathcal{R}_j} f(z \mid \mathcal{H}_i) \mathrm{d}z, \tag{14}$$

which corresponds to $P(\bar{z}_j \mid \bar{c}_{m_{\mathcal{K}}})$ by reverse mapping $m_k \mapsto i$. In summary, with the CSI knowledge and for any given precoder and detection threshold set, we can obtain the expected power of the received signal per block by (6), the conditional probability density function of the accumulated energy by (7), the corresponding decision region by (**??**), and the equivalent point-to-point channel by (14).

C. Sum backscatter rate

We first introduce some prerequisites of information theory. Define the input probability distribution of tag k at state m_k as $P_k(\bar{c}_{m_k})$, and let $\boldsymbol{p}_k \triangleq [P_k(\bar{c}_1), \ldots, P_k(\bar{c}_M)]^T \in \mathbb{R}^{M \times 1}$, $\boldsymbol{P} \triangleq [\boldsymbol{p}_1^T, \ldots, \boldsymbol{p}_K^T]^T \in \mathbb{R}^{M \times K}$. Assume the input distribution of all tags are mutually independent such that the probability associated with input combination $\bar{c}_{m_{\mathcal{K}}}$ satisfies $P_{\mathcal{K}}(\bar{c}_{m_{\mathcal{K}}}) = \prod_{k \in \mathcal{K}} P_k(\bar{c}_{m_k})$. Following [15], the corresponding backscatter information function is defined as

$$I_{\mathrm{B}}(\bar{c}_{m_{\mathcal{K}}}; z) \triangleq \sum_j P(\bar{z}_j \mid \bar{c}_{m_{\mathcal{K}}}) \log \frac{P(\bar{z}_j \mid \bar{c}_{m_{\mathcal{K}}})}{P(\bar{z}_j)}, \tag{15}$$

where $P(\bar{z}_j) = \sum_{m_{\mathcal{K}}} P_{\mathcal{K}}(\bar{c}_{m_{\mathcal{K}}}) P(\bar{z}_j \mid \bar{c}_{m_{\mathcal{K}}})$. The backscatter marginal information function of tag $k \in \mathcal{K}$ associated with $\bar{c}_{m_k}$, $m_k \in \mathcal{M}$ is defined as

$$I_{\mathrm{B},k}(\bar{c}_{m_k}; z) \triangleq \sum_{m_{\mathcal{K} \setminus \{k\}}} P_{\mathcal{K} \setminus \{k\}}(\bar{c}_{m_{\mathcal{K} \setminus \{k\}}}) I_{\mathrm{B}}(\bar{c}_{m_{\mathcal{K} \setminus \{k\}}}, \bar{c}_{m_k}; z), \tag{16}$$

where $P_{\mathcal{K} \setminus \{k\}}(\bar{c}_{m_{\mathcal{K} \setminus \{k\}}}) = \prod_{q \in \mathcal{K} \setminus \{k\}} P_q(\bar{c}_{m_q})$. The backscatter mutual information can be expressed as[11]

$$I_{\mathrm{B}}(c_{\mathcal{K}}; z) = \mathbb{E}_{c_{\mathcal{K}}}\left[I_{\mathrm{B}}(\bar{c}_{m_{\mathcal{K}}}; z)\right] = \mathbb{E}_{c_k}\left[I_{\mathrm{B},k}(\bar{c}_{m_k}; z)\right] \tag{17a}$$

$$= \sum_{m_{\mathcal{K}}} P_{\mathcal{K}}(\bar{c}_{m_{\mathcal{K}}}) \sum_j P(\bar{z}_j \mid \bar{c}_{m_{\mathcal{K}}}) \log \frac{P(\bar{z}_j \mid \bar{c}_{m_{\mathcal{K}}})}{P(\bar{z}_j)}. \tag{17b}$$

Evidently, (15)–(17) are functions of the tag input distribution $\boldsymbol{P}$ as well as the discrete memoryless MAC $P(z \mid c_{\mathcal{K}})$, and thus depend on the transmit precoder $\boldsymbol{w}$ and the detection threshold $\boldsymbol{t}$.

D. Ergodic primary rate

Once the tag input combination is successfully decoded, the user can eliminate backscatter uncertainty and model its contribution within the equivalent primary channel (5). As such, the tags can adjust the propagation environment in a potentially

[8] We consider strict inequality in the definition, as otherwise S and $\boldsymbol{t}$ could be non-unique for a given thresholding scheme.

[9] The proof holds for general mapping $R_s \mapsto \mathcal{R}_j$, and we focus on this specific case for the ease of notation.

[10] For simplicity, we assume there exists at least one feasible precoder that produces distinct received energy levels for all tag input combinations. [TODO] Merge with precoder design.

[11] Please be aware that $c_{\mathcal{K}}$, c_k, z are random variables, while $\bar{c}_{m_{\mathcal{K}}}$ and $\bar{c}_i$, $\bar{c}_{m_k}$, $\bar{z}_j$ represent the corresponding instances.

beneficial manner, and create artificial channel variation within each fading block. Similarly, we define the primary information function associated with tag input combination $\bar{c}_{m_\mathcal{K}}$ and the primary marginal information function of tag k associated with symbol $\bar{c}_{m_k}$ respectively as

$$I_\mathrm{P}(\bar{c}_{m_\mathcal{K}};\boldsymbol{y}) \triangleq N\log_2\left(1+\frac{|\boldsymbol{h}_\mathrm{E}^H(\bar{c}_{m_\mathcal{K}})\boldsymbol{w}|^2}{\sigma_w^2}\right), \tag{18}$$

$$I_{\mathrm{P},k}(\bar{c}_{m_k};\boldsymbol{y}) \triangleq \sum_{m_{\mathcal{K}\setminus\{k\}}} P_{\mathcal{K}\setminus\{k\}}(\bar{c}_{m_{\mathcal{K}\setminus\{k\}}}) I_\mathrm{P}(\bar{c}_{m_{\mathcal{K}\setminus\{k\}}},\bar{c}_{m_k};\boldsymbol{y}), \tag{19}$$

and the ergodic primary rate can be expressed as[12]

$$I_\mathrm{P}(c_\mathcal{K};\boldsymbol{y}) = \mathbb{E}_{c_\mathcal{K}}\left[I_\mathrm{P}(\bar{c}_{m_\mathcal{K}};\boldsymbol{y})\right] = \mathbb{E}_{c_k}\left[I_{\mathrm{P},k}(\bar{c}_{m_k};\boldsymbol{y})\right] \tag{20a}$$

$$= \sum_{m_\mathcal{K}} P_\mathcal{K}(\bar{c}_{m_\mathcal{K}}) N\log_2\left(1+\frac{|\boldsymbol{h}_\mathrm{E}^H(\bar{c}_{m_\mathcal{K}})\boldsymbol{w}|^2}{\sigma_w^2}\right). \tag{20b}$$

In contrast to the backscatter case, (18)–(20) are irrelevant to the detection threshold $\boldsymbol{t}$, but depend on the tag input probability distribution $\boldsymbol{P}$ and the transmit precoder $\boldsymbol{w}$.

III. Input Distribution, Decision Region, and Precoder Design

A. Primary-backscatter rate region

Define the weighted sum information function associated with tag input combination $\bar{c}_{m_\mathcal{K}}$ as

$$I(\bar{c}_{m_\mathcal{K}};\boldsymbol{y},z) \triangleq \rho I_\mathrm{P}(\bar{c}_{m_\mathcal{K}};\boldsymbol{y}) + (1-\rho) I_\mathrm{B}(\bar{c}_{m_\mathcal{K}};z), \tag{21}$$

the weighted sum marginal information of tag k associated with symbol $\bar{c}_{m_k}$ as

$$I_k(\bar{c}_{m_k};\boldsymbol{y},z) \triangleq \rho I_{\mathrm{P},k}(\bar{c}_{m_k};\boldsymbol{y}) + (1-\rho) I_{\mathrm{B},k}(\bar{c}_{m_k};z), \tag{22}$$

and the weighted sum primary-backscatter rate as

$$I(c_\mathcal{K};\boldsymbol{y},z) \triangleq \rho I_\mathrm{P}(c_\mathcal{K};\boldsymbol{y}) + (1-\rho) I_\mathrm{B}(c_\mathcal{K};z), \tag{23}$$

where $\rho \in [0,1]$ denotes the priority of the primary link. To investigate how backscatter modulation and detection may influence the primary transmission, we optimize the input probability distribution, decision region, and transmit precoder to maximize the weighted sum primary-backscatter rate

$$\max_{\boldsymbol{P},\boldsymbol{t},\boldsymbol{w}} \quad I(c_\mathcal{K};\boldsymbol{y},z) \tag{24a}$$

$$\text{s.t.} \quad \textstyle\sum_{m_k} P_k(\bar{c}_{m_k}) = 1, \quad \forall k\in\mathcal{K}, \tag{24b}$$

$$P_k(\bar{c}_{m_k}) \geq 0, \quad \forall m_k\in\mathcal{M},\ \forall k\in\mathcal{K}, \tag{24c}$$

$$\|\boldsymbol{w}\|^2 \leq P. \tag{24d}$$

where (24b) and (24c) are input probability constraints and (24d) is the average transmit power budget. As problem (24) is not jointly convex over $\boldsymbol{P}$, $\boldsymbol{t}$ and $\boldsymbol{w}$, we propose a Block Coordinate Descent (BCD) method that iteratively updates the input distribution, decision region, and transmit precoder, until convergence is achieved.

[12]The unit of (15)–(17) are bit per channel use (bpcu), while the unit of (18)–(20) are bit per second per Hertz (bps/Hz).

B. Input probability distribution

For any fixed decision boundary $\boldsymbol{t}$ and transmit precoder $\boldsymbol{w}$, the equivalent discrete memoryless MAC can be determined by (14) and problem (24) boils down to

$$\max_{\boldsymbol{P}} \quad I(c_\mathcal{K};\boldsymbol{y},z) \tag{25a}$$

$$\text{s.t.} \quad (24\text{b}),(24\text{c}), \tag{25b}$$

which is non-convex for $K>1$ due to the product term $\prod_{k\in\mathcal{K}} P_k(\bar{c}_{m_k})$. Fortunately, the KKT conditions are necessary and sufficient for this type of problem, and the proof follows straightforwardly from [16].[13]

Proposition 1. *The necessary and sufficient conditions for an input probability distribution $\boldsymbol{P}^\star$ to maximize the weighted sum primary-backscatter rate are that, $\forall m_k\in\mathcal{M}$ and $\forall k\in\mathcal{K}$,*

$$I_k^\star(\bar{c}_{m_k};\boldsymbol{y},z) = I^\star(c_\mathcal{K};\boldsymbol{y},z), \quad P_k^\star(\bar{c}_{m_k}) > 0, \tag{26a}$$

$$I_k^\star(\bar{c}_{m_k};\boldsymbol{y},z) \leq I^\star(c_\mathcal{K};\boldsymbol{y},z), \quad P_k^\star(\bar{c}_{m_k}) = 0. \tag{26b}$$

(26a) *means each probable state of each tag should produce the same marginal information (averaged over all states of other tags), while* (26b) *implies any state of any tag with potentially less marginal information than above should not be used.*

Proof. Denote the Lagrange multiplier associated with (24b) and (24c) as $\boldsymbol{\nu} \triangleq [\nu_1,\ldots,\nu_K]^T \in \mathbb{R}^{K\times 1}$ and $\boldsymbol{\Lambda} \triangleq [\boldsymbol{\lambda}_1^T,\ldots,\boldsymbol{\lambda}_K^T]^T \in \mathbb{R}^{M\times K}$ with $\boldsymbol{\lambda}_k \triangleq [\lambda_{k,1},\ldots,\lambda_{k,M}]^T \in \mathbb{R}^{M\times 1}$, respectively. The Lagrangian function of problem (25) is

$$L(\boldsymbol{P},\boldsymbol{\nu},\boldsymbol{\Lambda}) = -I(c_\mathcal{K};\boldsymbol{y},z) + \sum_{k\in\mathcal{K}} \nu_k\left(\sum_{m_k\in\mathcal{M}} P_k(\bar{c}_{m_k}) - 1\right) - \sum_{k\in\mathcal{K}}\sum_{m_k\in\mathcal{M}} \lambda_{k,m_k} P_k(\bar{c}_{m_k}), \tag{27}$$

and the corresponding KKT conditions are, $\forall m_k\in\mathcal{M}$ and $\forall k\in\mathcal{K}$,

$$-\nabla_{P_k^\star(\bar{c}_{m_k})} I^\star(c_\mathcal{K};\boldsymbol{y},z) + \nu_k^\star - \lambda_{k,m_k}^\star = 0, \tag{28a}$$

$$\lambda_{k,m_k}^\star = 0, \quad P_k^\star(\bar{c}_{m_k}) > 0, \tag{28b}$$

$$\lambda_{k,m_k}^\star \geq 0, \quad P_k^\star(\bar{c}_{m_k}) = 0, \tag{28c}$$

where the directional derivative can be explicitly expressed as

$$\nabla_{P_k^\star(\bar{c}_{m_k})} I^\star(c_\mathcal{K};\boldsymbol{y},z) = I_k^\star(\bar{c}_{m_k};\boldsymbol{y},z) - (1-\rho). \tag{29}$$

Due to the necessity and sufficiency of the KKT conditions, we conclude that any input probability distribution $\boldsymbol{P}^\star$ maximizes the weighted sum primary-backscatter rate if and only if, $\forall m_k\in\mathcal{M}$ and $\forall k\in\mathcal{K}$,

$$I_k^\star(\bar{c}_{m_k};\boldsymbol{y},z) = \nu_k^\star + (1-\rho), \quad P_k^\star(\bar{c}_{m_k}) > 0, \tag{30a}$$

$$I_k^\star(\bar{c}_{m_k};\boldsymbol{y},z) \leq \nu_k^\star + (1-\rho), \quad P_k^\star(\bar{c}_{m_k}) = 0, \tag{30b}$$

[13]For any elementary discrete memoryless MAC (sizes of input alphabets are no greater than that of output alphabet), the sufficiency can be proved by combining the local maximum and connectedness of KKT solutions. For any general discrete memoryless MAC, the capacity can be achieved by an elementary discrete memoryless MAC included within. Thus, we restrict the discussion of this paper to elementary discrete memoryless MACs.

which implies

$$\sum_{m_k} P_k^\star(\bar{c}_{m_k}) I_k^\star(\bar{c}_{m_k};\boldsymbol{y},z) = \nu_k^\star + (1-\rho). \tag{31}$$

On the other hand, by definition of marginations (17a), (20a) and weighted summations (22), (23), we have

$$\sum_{m_k} P_k^\star(\bar{c}_{m_k}) I_k^\star(\bar{c}_{m_k};\boldsymbol{y},z) = I^\star(c_{\mathcal{K}};\boldsymbol{y},z), \tag{32}$$

which is irrelevant to k. It suggests $I^\star(c_{\mathcal{K}};\boldsymbol{y},z) = \nu_k^\star + (1-\rho)$, $\forall k \in \mathcal{K}$, and completes the proof. □

Next, we extend the Blahut-Arimoto algorithm to the proposed case and obtain the optimal input probability distribution as follows.

Theorem 2. *The input probability distribution that achieves the weighted sum primary-backscatter capacity, at state $m_k \in \mathcal{M}$ of tag $k \in \mathcal{K}$, is given by the converging point of sequence*[14]

$$P_k^{(r+1)}(\bar{c}_{m_k}) = \frac{P_k^{(r)}(\bar{c}_{m_k}) \exp\left(\frac{\rho}{1-\rho} I_k^{(r)}(\bar{c}_{m_k};\boldsymbol{y},z)\right)}{\sum_{m_k'} P_k^{(r)}(\bar{c}_{m_k'}) \exp\left(\frac{\rho}{1-\rho} I_k^{(r)}(\bar{c}_{m_k'};\boldsymbol{y},z)\right)}, \tag{33}$$

where $r \in \mathbb{Z}_+$ is the iteration index and $P_k^{(0)}(\bar{c}_{m_k}) > 0$.

Proof. We first prove sequence (33) is non-decreasing in mutual information. For state $m_k \in \mathcal{M}$ of tag $k \in \mathcal{K}$, let $P_{\mathcal{K}}(\bar{c}_{m_{\mathcal{K}}}) = \prod_{q\in\mathcal{K}} P_q(\bar{c}_{m_q})$ and $P'_{\mathcal{K}}(\bar{c}_{m_{\mathcal{K}}}) = P'_k(\bar{c}_{m_k}) \prod_{q\in\mathcal{K}\setminus\{k\}} P_q(\bar{c}_{m_q})$ be two probability distributions with potentially different marginal for tag k, and define an intermediate function $J\left(P_{\mathcal{K}}(\bar{c}_{m_{\mathcal{K}}}), P'_{\mathcal{K}}(\bar{c}_{m_{\mathcal{K}}})\right)$ by (34). Apparently, $I(\bar{c}_{\mathcal{K}};\boldsymbol{y},z) = J\left(P_{\mathcal{K}}(\bar{c}_{m_{\mathcal{K}}}), P_{\mathcal{K}}(\bar{c}_{m_{\mathcal{K}}})\right)$. For a fixed $P'_{\mathcal{K}}(\bar{c}_{m_{\mathcal{K}}})$, $J\left(P_{\mathcal{K}}(\bar{c}_{m_{\mathcal{K}}}), P'_{\mathcal{K}}(\bar{c}_{m_{\mathcal{K}}})\right)$ is a concave function of $P_k(\bar{c}_{m_k})$ and is maximized at $\nabla_{P_k^\star(\bar{c}_{m_k})} J\left(P_{\mathcal{K}}(\bar{c}_{m_{\mathcal{K}}}), P'_{\mathcal{K}}(\bar{c}_{m_{\mathcal{K}}})\right) = 0$, namely

$$S'_k(\bar{c}_{m_k}) - S'_k(\bar{c}_{i_k}) + (1-\rho)\log\frac{P_k(\bar{c}_{i_k})}{P_k^\star(\bar{c}_{m_k})} = 0, \tag{35}$$

where $i_k \neq m_k$ is the reference state and

$$S'_k(\bar{c}_{m_k}) \triangleq I'_k(\bar{c}_{m_k};\boldsymbol{y},z) + (1-\rho)\sum_{m_{\mathcal{K}\setminus\{k\}}} P_{\mathcal{K}\setminus\{k\}}(\bar{c}_{m_{\mathcal{K}\setminus\{k\}}}) \times \sum_j P(\bar{z}_j \mid \bar{c}_{m_{\mathcal{K}\setminus\{k\}}}, \bar{c}_{m_k}) \log P'_{\mathcal{K}}(\bar{c}_{m_{\mathcal{K}\setminus\{k\}}}, \bar{c}_{m_k}). \tag{36}$$

[14]Note that the probability distribution of tag k is based on the updated probability distribution of tags $1,\ldots,k-1$.

Evidently, $\forall m_k \neq i_k$, (35) boils down to

$$\begin{aligned} P_k^\star(\bar{c}_{m_k}) &= \frac{\exp\left(\frac{1}{1-\rho} S'_k(\bar{c}_{m_k})\right)}{\sum_{m_k'} \exp\left(\frac{1}{1-\rho} S'_k(\bar{c}_{m_k'})\right)} &\text{(37a)}\\ &= \frac{P'_k(\bar{c}_{m_k}) u'_k(\bar{c}_{m_k})}{\sum_{m_k'} P'_k(\bar{c}_{m_k'}) u'_k(\bar{c}_{m_k'})}, &\text{(37b)}\end{aligned}$$

where we define $u'_k(\bar{c}_{m_k}) \triangleq \exp\left(\frac{\rho}{1-\rho} I'_k(\bar{c}_{m_k};\boldsymbol{y},z)\right)$. Although $P_k(\bar{c}_{i_k}) = 1 - \sum_{m_k\neq i_k} P_k^\star(\bar{c}_{m_k})$ is not guaranteed to be optimal, it has exactly the same form as (37b). In such case, the solution of choosing i_k as reference would coincide with that of choosing any $m_k \neq i_k$ as reference, while optimality for i_k is guaranteed in the latter case. Therefore, for a fixed $P'_{\mathcal{K}}(\bar{c}_{m_{\mathcal{K}}})$, $\forall i_k \in \mathcal{M}$ and $\forall k \in \mathcal{K}$, (37b) ensures

$$J\left(P_{\mathcal{K}}(\bar{c}_{m_{\mathcal{K}}}), P'_{\mathcal{K}}(\bar{c}_{m_{\mathcal{K}}})\right) \geq I'(\bar{c}_{\mathcal{K}};\boldsymbol{y},z). \tag{38}$$

On the other hand, choosing $P_k(\bar{c}_{m_k})$ by (37b) also satisfies

$$\begin{aligned}
\Delta &\triangleq I(\bar{c}_{\mathcal{K}};\boldsymbol{y},z) - J\left(P_{\mathcal{K}}(\bar{c}_{m_{\mathcal{K}}}), P'_{\mathcal{K}}(\bar{c}_{m_{\mathcal{K}}})\right) &\text{(39a)}\\
&= (1-\rho)\sum_{m_{\mathcal{K}}} P_{\mathcal{K}}(\bar{c}_{m_{\mathcal{K}}}) \sum_j P(\bar{z}_j \mid \bar{c}_{m_{\mathcal{K}}}) \log\frac{P'(\bar{z}_j) P_k(\bar{c}_{m_k})}{P(\bar{z}_j) P'_k(\bar{c}_{m_k})} &\text{(39b)}\\
&= (1-\rho)\sum_{m_k} \frac{P'_k(\bar{c}_{m_k}) u'_k(\bar{c}_{m_k})}{\sum_{m_k'} P'_k(\bar{c}_{m_k'}) u'_k(\bar{c}_{m_k'})} \sum_j P(\bar{z}_j \mid \bar{c}_{m_k}) \\
&\quad \times \log\frac{\sum_{m_k'} P'_k(\bar{c}_{m_k'}) P(\bar{z}_j \mid \bar{c}_{m_k'}) u'_k(\bar{c}_{m_k})}{\sum_{m_k'} P'_k(\bar{c}_{m_k'}) P(\bar{z}_j \mid \bar{c}_{m_k'}) u'_k(\bar{c}_{m_k'})} &\text{(39c)}\\
&\geq (1-\rho)\sum_{m_k} \frac{P'_k(\bar{c}_{m_k}) u'_k(\bar{c}_{m_k})}{\sum_{m_k'} P'_k(\bar{c}_{m_k'}) u'_k(\bar{c}_{m_k'})} \sum_j P(\bar{z}_j \mid \bar{c}_{m_k}) \\
&\quad \times \left(1 - \frac{\sum_{m_k'} P'_k(\bar{c}_{m_k'}) P(\bar{z}_j \mid \bar{c}_{m_k'}) u'_k(\bar{c}_{m_k'})}{\sum_{m_k'} P'_k(\bar{c}_{m_k'}) P(\bar{z}_j \mid \bar{c}_{m_k'}) u'_k(\bar{c}_{m_k})}\right) &\text{(39d)}\\
&= 0, &\text{(39e)}
\end{aligned}$$

where the equality holds if and only if (37b) converges. Combining (38) and (39) suggests $I(\bar{c}_{\mathcal{K}};\boldsymbol{y},z) \geq I'(\bar{c}_{\mathcal{K}};\boldsymbol{y},z)$. Since mutual information is bounded above, we conclude sequence (33) is non-decreasing and convergent in mutual information.

We then prove any converging point of sequence (33), denoted as $P_k^\star(\bar{c}_{m_k})$, fulfills the optimal conditions (26) and achieves the weighted primary-backscatter sum capacity. To see this, define

$$D_k^{(r)}(\bar{c}_{m_k}) \triangleq \frac{P_k^{(r+1)}(\bar{c}_{m_k})}{P_k^{(r)}(\bar{c}_{m_k})} = \frac{u_k^{(r)}(\bar{c}_{m_k})}{\sum_{m_k'} P_k^{(r)}(\bar{c}_{m_k'}) u_k^{(r)}(\bar{c}_{m_k'})}, \tag{40}$$

$$\begin{aligned} J\left(P_{\mathcal{K}}(\bar{c}_{m_{\mathcal{K}}}), P'_{\mathcal{K}}(\bar{c}_{m_{\mathcal{K}}})\right) &\triangleq \rho\sum_{m_{\mathcal{K}}} P_{\mathcal{K}}(\bar{c}_{m_{\mathcal{K}}}) N \log_2\left(1 + \frac{|\boldsymbol{h}_{\mathrm{E}}^H(\bar{c}_{m_{\mathcal{K}}})\boldsymbol{w}|^2}{\sigma_w^2}\right) \\ &\quad + (1-\rho)\sum_{m_{\mathcal{K}}} P_{\mathcal{K}}(\bar{c}_{m_{\mathcal{K}}}) \sum_j P(\bar{z}_j \mid \bar{c}_{m_{\mathcal{K}}}) \log\frac{P(\bar{z}_j \mid \bar{c}_{m_{\mathcal{K}}}) P'_{\mathcal{K}}(\bar{c}_{m_{\mathcal{K}}})}{P'(\bar{z}_j) P_{\mathcal{K}}(\bar{c}_{m_{\mathcal{K}}})}. \end{aligned} \tag{34}$$

where $P_k^{(0)}(\bar{c}_{m_k}) > 0$. As sequence (33) is convergent, any state with $P_k^\star(\bar{c}_{m_k}) > 0$ need to satisfy $D_k^\star(\bar{c}_{m_k}) \triangleq \lim_{r\to\infty} D_k^{(r)}(\bar{c}_{m_k}) = 1$, namely

$$I_k^\star(\bar{c}_{m_k}; \boldsymbol{y}, z) = \frac{1-\rho}{\rho} \log \sum_{m_k'} P_k^\star(\bar{c}_{m_k'}) u_k^\star(\bar{c}_{m_k'}), \tag{41}$$

which coincides with (30a) and implies (26a). That is, given $P_k^{(0)}(\bar{c}_{m_k}) > 0$, any converging point with $P_k^\star(\bar{c}_{m_k}) > 0$ must satisfy (26a). On the other hand, we assume $P_k^\star(\bar{c}_{m_k})$ does not satisfy (26b), such that for any state with $P_k^\star(\bar{c}_{m_k}) = 0$,

$$I_k^\star(\bar{c}_{m_k}; \boldsymbol{y}, z) > I^\star(c_{\mathcal{K}}; \boldsymbol{y}, z) = \sum_{m_k'} P_k^\star(\bar{c}_{m_k'}) I_k^\star(\bar{c}_{m_k'}; \boldsymbol{y}, z), \tag{42}$$

where the equality origins from (17a) and (20a). Since the exponential function is monotonically increasing, we have $u_k^\star(\bar{c}_{m_k}) > \sum_{m_k'} P_k^\star(\bar{c}_{m_k'}) u_k^\star(\bar{c}_{m_k'})$ and $D_k^\star(\bar{c}_{m_k}) > 1$. Considering $P_k^{(0)}(\bar{c}_{m_k}) > 0$ and $P_k^\star(\bar{c}_{m_k}) = 0$, it contradicts with

$$P_k^{(r)}(\bar{c}_{m_k}) = P_k^{(0)}(\bar{c}_{m_k}) \prod_{n=1}^{r} D_k^{(n)}(\bar{c}_{m_k}). \tag{43}$$

Therefore, given $P_k^{(0)}(\bar{c}_{m_k}) > 0$, any converging point with $P_k^\star(\bar{c}_{m_k}) = 0$ must satisfy (26b).

In conclusion, sequence (33) always converges to a weighted sum capacity-achieving distribution for state m_k of tag k. $\square$

C. Decision region

As indicated by [17], the optimal Maximum-Likelihood (ML) decision regions are very close to the optimal decision regions to problem (24). We can either use (**??**) as suboptimal, or take derivative of (17) w.r.t. $t_{i-1,i}$ and $t_{i,i+1}$ (however, closed-form solutions are unavailable and two-dimensional search is needed).

D. Precoder

Interestingly, we can design precoder to adjust the expectation of the received power (6) at each tag input combination, which can avoid the detection blind spots in [11] and further boost the weighted sum-rate. However, the problem is highly non-convex – the information function associated with input combination state i is

$$\begin{aligned} I(\bar{c}_i; z) = \sum_{j\in\mathcal{I}} \int_{t_{j-1,j}}^{t_{j,j+1}} \frac{z^{N-1} \exp\left(-\frac{z}{\mathrm{tr}(H_{\mathrm{E},i}W)+\sigma_w^2}\right)}{\left(\mathrm{tr}(H_{\mathrm{E},i}W)+\sigma_w^2\right)^N (N-1)!} \mathrm{d}z \\ \times \log \frac{\int_{t_{j-1,j}}^{t_{j,j+1}} \frac{z^{N-1} \exp\left(-\frac{z}{\mathrm{tr}(H_{\mathrm{E},i}W)+\sigma_w^2}\right)}{\left(\mathrm{tr}(H_{\mathrm{E},i}W)+\sigma_w^2\right)^N (N-1)!} \mathrm{d}z}{\sum_{i'\in\mathcal{I}} \int_{t_{j-1,j}}^{t_{j,j+1}} \frac{z^{N-1} \exp\left(-\frac{z}{\mathrm{tr}(H_{\mathrm{E},i'}W)+\sigma_w^2}\right)}{\left(\mathrm{tr}(H_{\mathrm{E},i'}W)+\sigma_w^2\right)^N (N-1)!} \mathrm{d}z}, \end{aligned} \tag{44}$$

and the mutual information can be expressed as a function of W by combining (17) and (44).

So far I have no idea how to solve this issue, and found no reference regarding precoder design for AmBC/Symbiotic Radio (SR) with discrete channels (although some naive combiner designs are available for Binary-Input Binary-Output (BIBO)). Personally, I believe the precoder design is the key to (i) boost the rate region and avoid blind spots in conventional AmBC; (ii) build our proposal over existing infrastructures. Ideally, assuming the number of transmit antennas Q is larger than the number of tags K, the optimal energy levels should be almost uniformly spaced (as z follows Erlang distribution) to concentrate the channel transitional probability on diagonal as possible.

References

[1] J. Kim and B. Clerckx, "Wireless Information and Power Transfer for IoT: Pulse Position Modulation, Integrated Receiver, and Experimental Validation," *arXiv:2104.08404*, pp. 1–15, apr 2021. [Online]. Available: http://arxiv.org/abs/2104.08404

[2] R. Hansen, "Relationships Between Antennas as Scatterers and as Radiators," *Proceedings of the IEEE*, vol. 77, no. 5, pp. 659–662, may 1989. [Online]. Available: http://ieeexplore.ieee.org/document/32056/

[3] C. Boyer and S. Roy, "Backscatter Communication and RFID: Coding, Energy, and MIMO Analysis," *IEEE Transactions on Communications*, vol. 62, no. 3, pp. 770–785, mar 2014. [Online]. Available: http://ieeexplore.ieee.org/document/6685977/

[4] Daniel Dobkin, *The RF in RFID: Passive UHF RFID in Practice*. London, U.K.: Newnes, nov 2012. [Online]. Available: https://www.elsevier.com/books/the-rf-in-rfid/dobkin/978-0-12-394583-9

[5] S. J. Thomas, E. Wheeler, J. Teizer, and M. S. Reynolds, "Quadrature Amplitude Modulated Backscatter in Passive and Semipassive UHF RFID Systems," *IEEE Transactions on Microwave Theory and Techniques*, vol. 60, no. 4, pp. 1175–1182, apr 2012. [Online]. Available: http://ieeexplore.ieee.org/document/6153042/

[6] D. Bharadia, K. R. Joshi, M. Kotaru, and S. Katti, "BackFi: High Throughput WiFi Backscatter," in *Proceedings of the 2015 ACM Conference on Special Interest Group on Data Communication*, vol. 45, no. 4. New York, NY, USA: ACM, aug 2015, pp. 283–296. [Online]. Available: https://dl.acm.org/doi/10.1145/2785956.2787490

[7] G. Yang, C. K. Ho, and Y. L. Guan, "Multi-Antenna Wireless Energy Transfer for Backscatter Communication Systems," *IEEE Journal on Selected Areas in Communications*, vol. 33, no. 12, pp. 2974–2987, dec 2015. [Online]. Available: http://ieeexplore.ieee.org/document/7274644/

[8] H. Guo, Q. Zhang, S. Xiao, and Y.-C. Liang, "Exploiting Multiple Antennas for Cognitive Ambient Backscatter Communication," *IEEE Internet of Things Journal*, vol. 6, no. 1, pp. 765–775, feb 2019. [Online]. Available: https://ieeexplore.ieee.org/document/8411483/

[9] Q. Wu and R. Zhang, "Intelligent Reflecting Surface Enhanced Wireless Network via Joint Active and Passive Beamforming," *IEEE Transactions on Wireless Communications*, vol. 18, no. 11, pp. 5394–5409, nov 2019. [Online]. Available: https://ieeexplore.ieee.org/document/8811733/

[10] H. Guo, Y.-C. Liang, R. Long, and Q. Zhang, "Cooperative Ambient Backscatter System: A Symbiotic Radio Paradigm for Passive IoT," *IEEE Wireless Communications Letters*, vol. 8, no. 4, pp. 1191–1194, aug 2019. [Online]. Available: https://ieeexplore.ieee.org/document/8692391/

[11] J. Qian, A. N. Parks, J. R. Smith, F. Gao, and S. Jin, "IoT Communications With M-PSK Modulated Ambient Backscatter: Algorithm, Analysis, and Implementation," *IEEE Internet of Things Journal*, vol. 6, no. 1, pp. 844–855, feb 2019. [Online]. Available: https://ieeexplore.ieee.org/document/8423609/

[12] T. Nguyen, Y.-J. Chu, and T. Nguyen, "On the Capacities of Discrete Memoryless Thresholding Channels," in *2018 IEEE 87th Vehicular Technology Conference (VTC Spring)*, vol. 2018-June. IEEE, jun 2018, pp. 1–5. [Online]. Available: https://ieeexplore.ieee.org/document/8417506/

[13] T. Nguyen and T. Nguyen, "Optimal Quantizer Structure for Maximizing Mutual Information Under Constraints," *IEEE Transactions on Communications*, vol. 69, no. 11, pp. 7406–7413, nov 2021. [Online]. Available: https://ieeexplore.ieee.org/document/9530430/

[14] T. D. Nguyen and T. Nguyen, "On Binary Quantizer For Maximizing Mutual Information," *IEEE Transactions on Communications*, vol. 68, no. 9, pp. 5435–5445, sep 2020. [Online]. Available: https://ieeexplore.ieee.org/document/9118952/

[15] M. Rezaeian and A. Grant, "Computation of Total Capacity for Discrete Memoryless Multiple-Access Channels," *IEEE Transactions on Information Theory*, vol. 50, no. 11, pp. 2779–2784, nov 2004. [Online]. Available: http://ieeexplore.ieee.org/document/1347364/

[16] Y. Watanabe and K. Kamoi, “A Formulation of the Channel Capacity of Multiple-Access Channel,” *IEEE Transactions on Information Theory*, vol. 55, no. 5, pp. 2083–2096, may 2009. [Online]. Available: http://ieeexplore.ieee.org/document/4839058/

[17] J. Qian, Y. Zhu, C. He, F. Gao, and S. Jin, “Achievable Rate and Capacity Analysis for Ambient Backscatter Communications,” *IEEE Transactions on Communications*, vol. 67, no. 9, pp. 6299–6310, sep 2019. [Online]. Available: https://ieeexplore.ieee.org/document/8721108/